MIT Libraries | DSpace@MIT

MIT Open Access Articles

Nanoengineered surfaces for microfluidic-based thermal management devices

The MIT Faculty has made this article openly available. ***Please share*** how this access benefits you. Your story matters.

Citation: Wang, Evelyn N., Rong Xiao, and Kuang-Han Chu. "Nanoengineered surfaces for microfluidic-based thermal management devices." Reliability, Packaging, Testing, and Characterization of MEMS/MOEMS and Nanodevices IX. Ed. Richard C. Kullberg & Rajeshuni Ramesham. San Francisco, California, USA: SPIE, 2010. 759202-7. ©2010 SPIE.

As Published: http://dx.doi.org/10.1117/12.842950

Publisher: SPIE

Persistent URL: http://hdl.handle.net/1721.1/58574

Version: Final published version: final published article, as it appeared in a journal, conference proceedings, or other formally published context

Terms of Use: Article is made available in accordance with the publisher's policy and may be subject to US copyright law. Please refer to the publisher's site for terms of use.

Massachusetts Institute of Technology

Invited Paper

Nanoengineered surfaces for microfluidic-based thermal management devices

Evelyn N. Wang*, Rong Xiao, Kuang-Han Chu
Device Research Laboratory, Department of Mechanical Engineering, MIT,
77 Massachusetts Ave., Cambridge, MA 02139

ABSTRACT

Microfluidic systems offer compact and efficient thermal management strategies. In this work, we investigate novel nanostructured surfaces to control fluidic behavior and enhance heat dissipation in microfluidic systems. We fabricated silicon nanopillars ranging from 200 nm to 800 nm in diameter and heights of approximately 5 μm. In the presence of notches on the pillars, the liquid separates into multiple layers of liquid films. The thicknesses of the liquid layers subsequently increase as the film propagates, which is determined by the specific position and geometry of the notches. In the presence of asymmetric nanopillars, where the pillars have deflection angles ranging from 0-50 degrees, directional spreading of water droplets can be achieved. The liquid spreads only in the direction of the pillar deflection and becomes pinned on the opposite interface. We performed detailed measurements and developed models to predict the behavior based on pillar geometries. These studies provide insight into the complex liquid-nanostructure interactions, which show great potential to design nanostructures to achieve high flux thermal management solutions.

Keywords: thermal management, nanoengineered surfaces, electronics cooling, microfluidics, heat sink

1. INTRODUCTION

The increasing heat generation rates in high performance electronic devices and systems are demanding the development of new thermal management solutions[1]. In particular, two-phase fluidic microfluidic cooling systems have received significant attention because the latent heat during liquid-vapor phase-change absorbs large fluxes with minimal changes in device temperature[2-4]. Efforts have focused primarily on boiling flows in microchannels. However, in these systems liquid-vapor instabilities during phase-change lead to local dry-out, non-uniform temperature distributions, and significant decreases in critical heat flux[5-9]. In contrast, two-phase jet impingement techniques have been investigated to a much lesser extent, despite the theoretical promise of very high heat transfer coefficients (>100 W/cm^{2}K) with high heat dissipation capability (>1000 W and >1000 W/cm^2) *via* thin film evaporation[2, 10]. Previous experimental attempts have typically led to pool boiling due to chamber flooding, or liquid dry-out due to insufficient liquid supply[2, 11]. These undesired effects significantly decreased heat transfer coefficients and heat removal rates.

Nanoengineered surfaces offer new opportunities to enhance and control fluid and heat transport for thin film evaporation. Significant efforts in past work focused on promoting nucleation sites by incorporating surface features and roughness to improve the critical heat flux in spray cooling[12-14] and pool boiling[15, 16]. Carbon nanotube (CNT) forests have more recently been investigated to enhance nucleate boiling and film boiling[17, 18]. In most of these studies, the surface features were neither sufficiently organized nor controlled. Recent progress in fabrication methods has enabled the creation of more defined and sophisticated micro-/nanoscale surface structures. For example, superhydrophobic surfaces using micro-/nanostructures have been explored to reduce drag[19, 20], to increase heat transfer coefficients by dropwise condensation[21], and to manipulate fluids and droplet directionalities[22, 23].

Controlled surface nanoengineering has also been recently researched to develop superhydrophilic surfaces for fluid wicking and liquid transport[24]. Efforts have focused on the effect of periodic simple structures on the liquid propagation and final wetted shape. In this work, we leverage three-dimensional nanostructured surface design to control fluidic behavior and to ultimately enhance heat dissipation in microfluidic systems.

Reliability, Packaging, Testing, and Characterization of MEMS/MOEMS and Nanodevices IX,
edited by Richard C. Kullberg, Rajeshuni Ramesham, Proc. of SPIE Vol. 7592, 759202
© 2010 SPIE · CCC code: 0277-786X/10/$18 · doi: 10.1117/12.842950

Downloaded from SPIE Digital Library on 02 Aug 2010 to 18.51.1.125. Terms of Use: http://spiedl.org/terms

2. FABRICATION AND CHARACTERIZATION OF NANOSTRUCTURED SURFACES

We designed and fabricated three-dimensional hydrophilic nanostructured surfaces to investigate the effect on liquid spreading. The nanostructures were fabricated in silicon, where the pillar diameters ranged from 200-800 nm with heights from 5-10 μm. The pillars were defined using projection lithography, and etched using deep reactive ion etching (DRIE). During the DRIE process, the etch and passivation cycles were varied to create intentional side scallops on the nanopillars, as shown in Fig. 1a. In addition, asymmetric nanostructures were fabricated, by subsequently depositing a thin film of gold on one side of the pillars, as shown in Fig. 1b. The thickness of the gold thin film determined the deflection angle, owing to the residual stresses between the two materials. The surfaces were then conformally coated with a hydrophilic polymer (where the contact angle of water on a polymer coated flat surface is 80°) to achieve uniform surface properties. The deflection angles ranged from 0-52 degrees.

Detailed studies of liquid behavior on the nanostructures were carried out. Deionized water (DI) with varying concentrations of surfactant (Triton X-100) ranging from 0.01% to 0.00125% by volume was used to vary the surface tension from 30.2 to 42.6 dynes/cm. Characterization techniques include environmental scanning electron microscopy, fluorescence and white light microscopy, and high speed imaging.

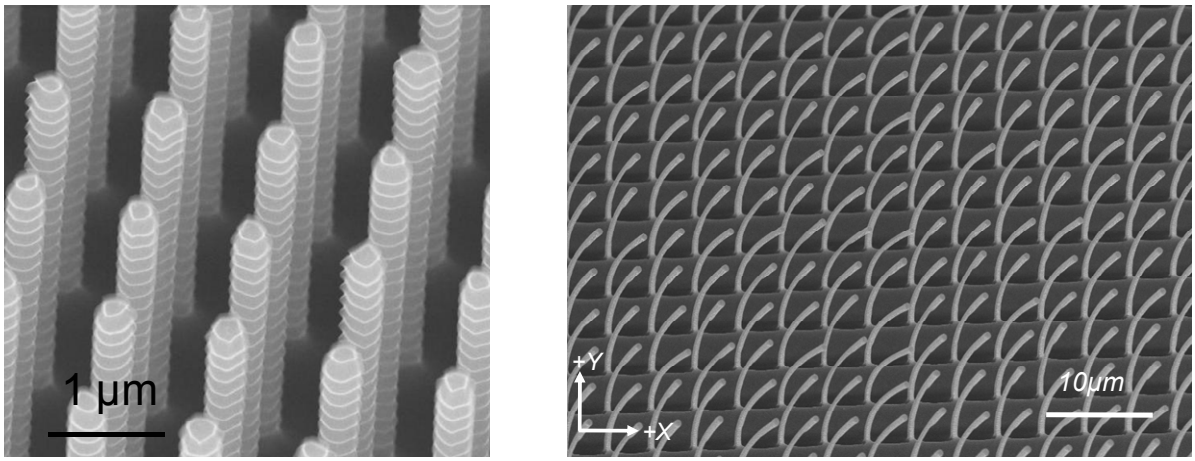

(a) (b)

Figure 1. Three-dimensional nanostructures fabricated in silicon. a) Nanopillars with notches on the sides of the features. b) Asymmetric nanostructures deflected at approximately 12 degrees.

We observed liquid separation into multiple layers during the propagation across surfaces with nanostructures as shown in the scanning electron micrograph (SEM) in Fig. 1a[25]. The pillars ranged in diameters from 500-800 nm and spacings from 500-800 nm. When a 2 μL droplet of DI water was deposited onto this surface, the liquid separated into several layers. A lower layer advanced first, and subsequent sequential layers followed on top of the first one. The phenomenon shown in Fig. 2 was visualized with fluorescent microscopy with a 40× magnification (NA=0.60). A 29 mM Rhodamine B solution was used to enhance the contrast between the visualized layers. The multi-layer separation was positively correlated to the presence of the scalloped features on the pillars. When pillar arrays with the same diameter and spacing were fabricated but with non-visible scalloped features, the liquid spread across the surface with a uniform thickness.

Downloaded from SPIE Digital Library on 02 Aug 2010 to 18.51.1.125. Terms of Use: http://spiedl.org/terms

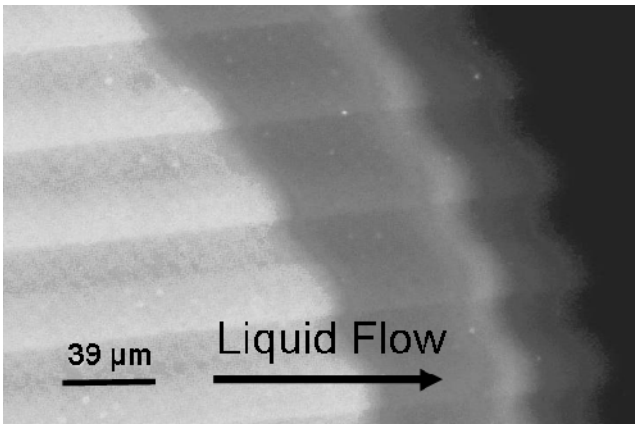

Figure 2. Fluorescent image showing that the liquid is separated into multiple layers during spreading on the pillars shown in Fig.1a.

We also studied the behavior of liquids on asymmetric nanostructures (Fig. 1b). Typical directional spreading behavior on the fabricated asymmetric nanostructures is shown in the time-lapse images of the side in Fig. 3. In this particular case, deionized (DI) water with a 0.002% concentration of surfactant (Triton X-100) by volume was deposited on the surface where the nanopillar deflection angle is 12°. The liquid propagates primarily towards the right, while the contact line pins in both the left and perpendicular directions (into the page).

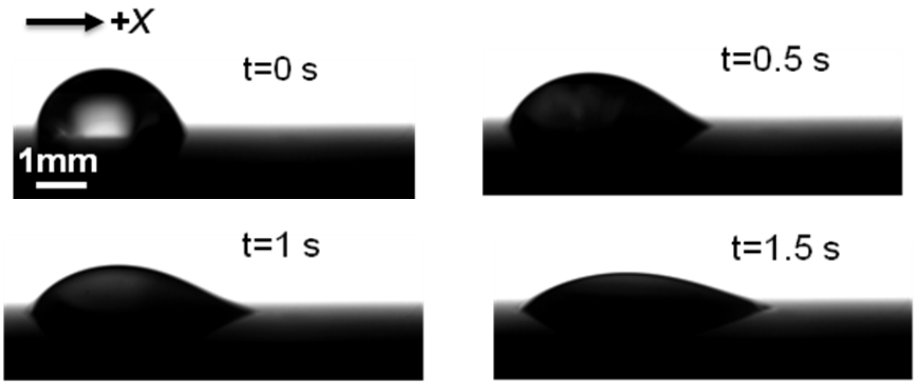

Figure 3. Time-lapse images of directional spreading of a liquid droplet. Side view of a 1 µL droplet of DI water with 0.002% by volume of Triton X-100 spreading on the surface corresponding to the asymmetric surface shown in Fig. 1b.

3. EXPERIMENTAL RESULTS AND DISCUSSIONS

We performed experiments and developed energy-based models to investigate the effect of three-dimensional geometries on liquid behavior. Based on our observations, the multi-layer liquid spreading was attributed to scallops of particular geometries that created energy barriers. A model based on surface energy was developed to explain the observations. In the model, the scallops are modeled as tiered steps as shown in Fig. 4(a).

Downloaded from SPIE Digital Library on 02 Aug 2010 to 18.51.1.125. Terms of Use: http://spiedl.org/terms

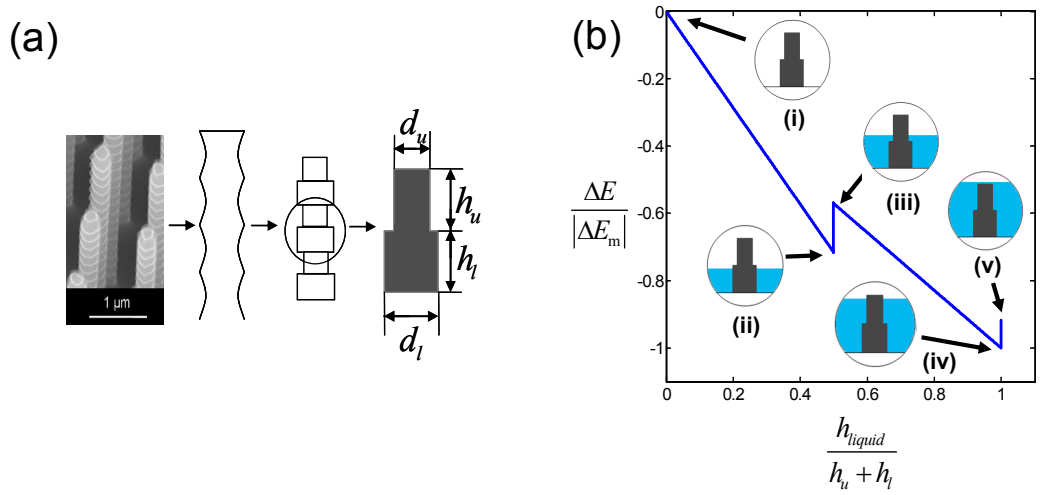

Figure 4. (a) Schematic showing a simplified model of the scalloped pillars from the DRIE process into tiered steps. (b) The change in normalized surface energy as a function of normalized liquid height on a two-tiered pillar geometry where h_u=h_l and d_u=$0.7d_l$.

The parameters h_u, h_l, d_u, d_l are the upper and lower height, and the upper and lower diameter, respectively. Fig. 4b shows the normalized change in surface energy as a function of the normalized liquid height. The pillars are hydrophilic, and therefore, a higher liquid height typically corresponds to a lower surface energy as shown between state (i) and state (ii), as well as between state (iii) and state (iv). However, in the presence of a horizontal surface, there is an energy barrier, as shown between state (ii) and state (iii). A similar energy barrier is present between state (iv) and state (v), which maintains the liquid below the top of the pillars. Fig. 4b shows a particular configuration with naturally oxidized silicon pillars with an intrinsic contact angle of 38 degrees, and with h_u=h_l and d_u =$0.7d_l$. The size of the energy barrier between state (ii) and state (iii) scales with the intrinsic contact angle and $1-(d_u/d_l)^2$. Therefore, for pillars of the same material (same intrinsic contact angle), a decrease in the d_u/d_l ratio will increase the size of this energy barrier such that state (iv) can have a higher energy than state (ii). The difference of the normalized energy between state (ii) and state (iv) plays an important role in the separation phenomena, which is determined by

$$S = \gamma_{LV}\frac{1}{h_u + h_l}\left(\frac{1}{\Lambda_1} - \frac{1}{C}\right) - \gamma_{LV}\frac{1}{h_u + h_l}\cos\theta\left(\frac{1}{\Lambda_1} - \frac{1}{C}\right) - \gamma_{LV}\frac{1}{l}\cos\theta\left(\frac{\pi A(C + B(1-C))}{\Lambda_2} - \frac{\pi A}{1 - \frac{\pi A^2}{4}}\right) \qquad (1)$$

where $\Lambda_1 = (1-C) + (1-\frac{\pi A^2}{4})C / (1-\frac{\pi A^2 B^2}{4})$, $\Lambda_2 = (1-\frac{\pi A^2 B^2}{4})(1-C) + (1-\frac{\pi A^2}{4})C$, A=d_l /l, B=d_u/d_l, C=$h_l/(h_u+h_l)$, l is the distance between the centers of neighboring pillars, and θ is the intrinsic contact angle of the liquid on the solid. When the liquid is deposited onto the surface, the liquid chooses the configuration with the lower surface energy. If S<0, the energy of state (ii) is lower than that of state (iv), and when a small volume of liquid, ΔV, is supplied from the droplet in this case, the liquid propagates at the edge as a separated layer. In contrast, when S>0, state (iv) is preferred because it has the lowest energy and the liquid remains in a uniform layer at the height of the pillars.

The analytical curve for S=0 as calculated from Eqn (1) is plotted in Fig. 5. For the case considered, γ_{LV}=0.072 N/m and θ =38 degrees, which results in C=0.49. The S=0 curve separate the regimes between single-layer and dual-layer spreading in the parameter space of A and B. To validate the model, additional pillars with a single notch of defined size, d_u, and location, h_l were fabricated. The experimental results are compared with the model predictions which show that the theoretical curve well demarcates the boundaries between geometries that lead to separated layers, and those that lead to a single layer, for both the advancing and receding processes. The results suggest that the spreading behavior can

Downloaded from SPIE Digital Library on 02 Aug 2010 to 18.51.1.125. Terms of Use: http://spiedl.org/terms

be controlled by choosing proper pillar geometries, which offer possibilities to control the thickness of liquid films on textured surfaces.

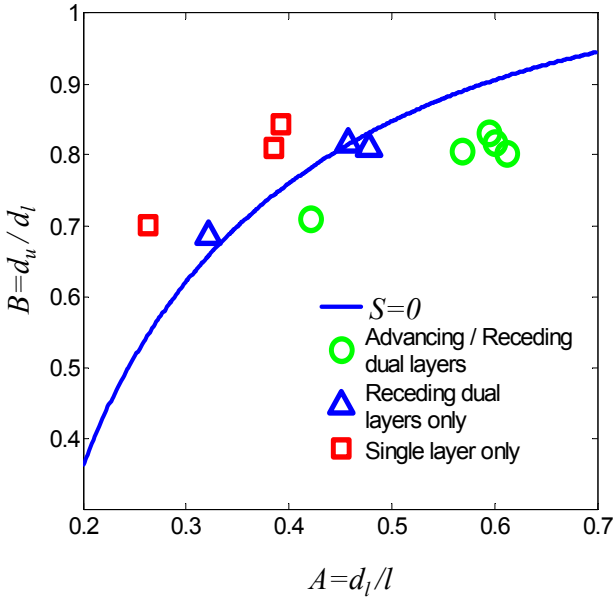

Figure 5. Parameter space that determines the presence of single or dual layers for the case C=0.49.

To achieve directional spreading work, the design of asymmetric structures, including the deflection angle, pillar height and spacing, and surface chemistry highly determines such behavior. We studied the liquid film that propagates ahead of the droplet within the nanopillars to elucidate the spreading behavior. The experimental results in Fig. 6 show the regimes by which the liquid propagates and pins as a function of the liquid intrinsic contact angle, θ_{in}, and pillar deflection angle, θ. The square symbols (□) indicate experiments in which the liquid film propagates only in the +X direction, whereas the crosses (□) are experiments where the film propagates in both +X and –X. The triangles (□) show instances where the liquid film is nearly pinned in the –X direction, *i.e.,* the propagating process was at least five times slower in –X than in +X. The behavior of the film along the Y-axis was similar to the behavior in the –X direction.

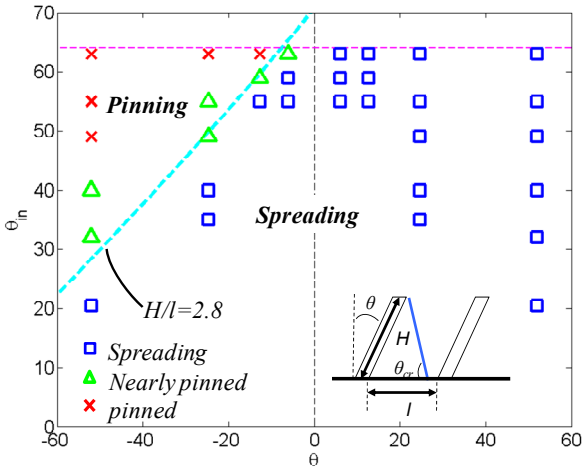

Figure 6. Experimental results showing regimes of directional liquid spreading.

Downloaded from SPIE Digital Library on 02 Aug 2010 to 18.51.1.125. Terms of Use: http://spiedl.org/terms

4. CONCLUSIONS

The work demonstrates that three-dimensional nanostructured surfaces can be designed and fabricated to achieve multi-layer liquid spreading and directional liquid spreading. A combined study of experiments and modeling efforts show the effect of nanopillar geometry and liquid surface tension on spreading behavior. The work offers insight into the design of nanostructures and exciting opportunities to achieve new manipulation capability for microfluidic-based thermal management systems.

5. ACKNOWLEDGMENTS

The authors gratefully acknowledge funding support from the National Science Foundation (under Award EEC-0824328), the DARPA Young Faculty Award, and the Northrop Grumman New Faculty Innovation Grant. The authors would also like to acknowledge the M.I.T. Microsystems Technology Lab for fabrication staff support, help, and use of equipment, Baris Erinc Polat from Prof. Blankschtein's group and Salmaan Baxamusa from Prof. Gleason's group in the Department of Chemical Engineering, M.I.T., for help with surface tension measurements and iCVD polymer deposition.

REFERENCES

[1] public.itrs.net
[2]Mudawar, I., "Assessment of high-heat-flux thermal management schemes," IEEE Transactions on Components & Packaging Technologies, 24(2), 122-141 (2001).
[3]Kandlikar, S. G. and Bapat, A. V., "Evaluation of jet impingement, spray and microchannel chip cooling options for high heat flux removal," Heat Transfer Engineering, 28(11), 911-923 (2007).
[4]Garimella, S. V., "Advances in mesoscale thermal management technologies for microelectronics," Microelectronics Journal, 37(11), 1165-1185 (2006).
[5]Bowers, M. B. and Mudawar, I., "High-flux boiling in low-flow rate, low-pressure drop mini-channel and microchannel heat sinks," International Journal of Heat and Mass Transfer, 37(2), 321-332 (1994).
[6]Kandlikar, S. G., "Fundamental issues related to flow boiling in minichannels and microchannels," Experimental Thermal and Fluid Science, 26(2-4), 389-407 (2002).
[7]Kandlikar, S. G., Kuan, W. K., Willistein, D. A. and Borrelli, J., "Stabilization of flow boiling in microchannels using pressure drop elements and fabricated nucleation sites," Journal of Heat Transfer, 128(4), 389-396 (2006).
[8]Qu, W. and Mudawar, I., "Measurement and correlation of critical heat flux in two-phase micro-channel heat sinks.," International Journal of Heat and Mass Transfer, 47(10/11), 2045-59 (2004).
[9]Zhang, L., Wang, E. N., Goodson, K. E. and Kenny, T. W., "Phase Change Phenomena in Silicon Microchannels," International Journal of Heat and Mass Transfer, 48(8), 1572-1582 (2005).
[10]Ohadi, M., Qi, J., and Lawler, J., [Ultra-Thin Film Evaporation (UTF) - Applications to Emergin Technologies in Cooling of Microelectronics, in Microscale Heat Transfer Fundamentals and Applications], Springer, Netherlands, 321-338 (2005).
[11]Wang, E. N., Zhang, L., Jiang, L., Koo, J.-M., Maveety, J. G., Sanchez, E. A., Goodson, K. E. and Kenny, T. W., "Micromachined Jets for Liquid Impingement of VLSI Chips," Journal of MicroElectroMechanical Systems, 13(5), 833-842 (2004).
[12]Silk, E. A., Kim, J. and Kiger, K., "Spray cooling of enhanced surfaces: Impact of structured surface geometry and spray axis inclination," International Journal Of Heat And Mass Transfer, 49(25-26), 4910-4920 (2006).
[13]Pais, M. R., Chow, L. C. and Mahefkey, E. T., "Surface-Roughness and Its Effects On The Heat-Transfer Mechanism In Spray Cooling," Journal Of Heat Transfer, 114(1), 211-219 (1992).
[14]Coursey, J. S., Kim, J. G. and Kiger, K. T., "Spray cooling of high aspect ratio open microchannels," Journal Of Heat Transfer, 129(8), 1052-1059 (2007).
[15]Murthy, S., Joshi, Y. and Nakayama, W., "Two-phase heat spreaders utilizing microfabricated boiling enhancement structures," Heat Transfer Engineering, 25(1), 26-36 (2004).
[16]Pal, A. and Joshi, Y., "Boiling of water at subatmospheric conditions with enhanced structures: Effect of liquid fill volume," Journal Of Electronic Packaging, 130(1), (2008).
[17]Ujereh, S., Fisher, T. and Mudawar, I., "Effects of carbon nanotube arrays on nucleate pool boiling," International Journal Of Heat And Mass Transfer, 50(19-20), 4023-4038 (2007).

Downloaded from SPIE Digital Library on 02 Aug 2010 to 18.51.1.125. Terms of Use: http://spiedl.org/terms

[18]Ahn, H. S., Sinha, N., Zhang, M., Banerjee, D., Fang, S. K. and Baughman, R. H., "Pool boiling experiments on multiwalled carbon nanotube (MWCNT) forests," Journal Of Heat Transfer, 128(12), 1335-1342 (2006).
[19]Choi, C. H. and Kim, C. J., "Large slip of aqueous liquid flow over a nanoengineered superhydrophobic surface," Physical Review Letters, 96(6), (2006).
[20]Ou, J. and Rothstein, J. P., "Direct velocity measurements of the flow past drag-reducing ultrahydrophobic surfaces," Physics Of Fluids, 17(10), (2005).
[21]Chen, C. H., Cai, Q. J., Tsai, C. L., Chen, C. L., Xiong, G. Y., Yu, Y. and Ren, Z. F., "Dropwise condensation on superhydrophobic surfaces with two-tier roughness," Applied Physics Letters, 90(17), (2007).
[22]Krupenkin, T. N., Taylor, J. A., Wang, E. N., Kolodner, P., Hodes, M. and Salamon, T. R., "Reversible Wetting-Dewetting Transitions on Electrically Tunable Superhydrophobic Nanostructured Surfaces," Langmuir, 23(18), 9128-9133 (2007).
[23]Shastry, A., Case, M. J. and Bohringer, K. F., "Directing droplets using microstructured surfaces," Langmuir, 22(14), 6161-6167 (2006).
[24]Courbin, L., Denieul, E., Dressaire, E., Roper, M., Ajdari, A. and Stone, H. A., "Imbibition by polygonal spreading on microdecorated surfaces," Nature Materials, 6(9), 661-664 (2007).
[25]Xiao, R., Chu, K. H. and Wang, E. N., "Multilayer liquid spreading on superhydrophilic nanostructured surfaces," Applied Physics Letters, 94(19), (2009).

Downloaded from SPIE Digital Library on 02 Aug 2010 to 18.51.1.125. Terms of Use: http://spiedl.org/terms